Synthesis, Structure, and Transport Properties of Novel Fullerides A_3C_{70} (A = Ba and Sm)

X. H. Chen,*,†,‡ D. H. Chi,‡ Z. Sun,† T. Takenobu,‡ Z. S. Liu,† and Y. Iwasa‡

Contribution from the Structure Research Laboratory and Department of Physics, University of Science and Technology of China, Hefei, Anhui 230026, P. R. China, and Japan Advanced Institute of Science and Technology, Tatsunokuchi, Ishikawa 923-1292, Japan

Received November 1, 1999

Abstract: A series of new stable fullerides A_3C_{70} (A = Sm, Ba) has been synthesized using solid-state reactions. The structure of Sm_3C_{70} has been identified to be monoclinic by simulation of synchrotron powder diffraction data. The structure of Ba_3C_{70} is derived from the A15 structure adopted by Ba_3C_{60}. The low symmetry relative to C_{60} fullerides could be an important factor in the absence of superconductivity in C_{70} fullerides. The electronic transport can be explained by a variable-range hopping mechanism for A_3C_{70} (A = Ba, Sm) samples, while the transport for Sm_xC_{70} ($x > 3$) samples appears to be dominated by weak localization (WL) theory.

Introduction

Many attempts to dope a wide variety of atoms or molecules into fullerenes have been made since the discovery of superconductivity in K_3C_{60} by Hebard et al.[1] It has been reported that alkali metals (K, Rb, Cs), alkali-earth metals (Ca, Sr, Ba), and rare-earth metals (Yb, Sm) can be intercalated into C_{60} solids.[1−9] Intercalation of these metals into C_{60} solids yields various structural compounds with different physical properties. Among these fullerides, Ba_3C_{60} has the A15 structure with a perfect alternating orientational order of the C_{60} molecules.[7] The basic structure of $R_{2.75}C_{60}$ (R = Yb, Sm) is face-centered cubic (fcc), but cation vacancy ordering in tetrahedral sites leads to a superstructure accompanied by a slight lattice deformation from cubic to orthorhombic.[8,9]

Due to their abundance in the conventional production process[10] the best investigated fullerenes are C_{60} and C_{70}. After the discovery of the C_{60}-derived fullerides (especially superconductivity in K_3C_{60}) it is, therefore, natural to look for similar fullerides in solid C_{70}. The question of how far C_{70} molecules differ chemically from C_{60} molecules has been debated in recent years in quite some detail.[11] At room temperature the spheroid-shaped C_{60} molecules adopt a fcc structure in which molecules are rotating. However, the crystal structure of the ellipsoid-shaped C_{70} is rather controversial. A fcc, a hexagonal closed-packed (hcp), a monoclinic, and a rhombohedral structure have been reported.[12,13] It is found that the equilibrium phase above room temperature is fcc, but that structural defects as well as residual solvent tend to stabilize the hcp phase.[12] Thus even highly pure C_{70} samples contain mixed-phase crystals consisting primarily of the fcc phase but also some hcp.

Relative to C_{60}, very little is known about the compounds of C_{70} so far, the next stable fullerene. The electronic structure has been reported for K-doped C_{70}[14] and for Rb-doped C_{70}.[15] Imaeda et al.[16] have used electron-spin resonance and microwave absorption to probe the electronic and magnetic properties of K_xC_{70}. Kobayashi et al.[17] reported a K-saturated fcc phase of K_9C_{70}, and the structure of K-doped C_{70} depended on the starting C_{70} structure. Electronic transport properties of K_xC_{70} thin films have been investigated by Wang et al.[18] No evidence of superconductivity has been reported and, to our knowledge, no

* To whom correspondence should be addressed.
† University of Science and Technology of China.
‡ Japan Advanced Institute of Science and Technology.

(1) Hebard, A. F.; Rosseinsky, M. J.; Haddon, R. C.; Murphy, D. W.; Glarum, S. H.; Palstra, T. T. M.; Ramirez, A. P.; Kortan, A. R. *Nature* **1991**, *350*, 600−601.
(2) Haddon, R. C.; Hebard, A. F.; Rosseinsky, M. J.; Murphy, D. W.; Duclos, S. J.; Lyons, K. B.; Miller, B.; Rosamilia, J. M.; Fleming, R. M.; Kortan, A. R.; Glarum, S. H.; Makhija, A. V.; Muller, A. J.; Eick, R. H.; Zahurak, S. M.; Tycko, R.; Dabbagh, G.; Thiel, F. A. *Nature* **1991**, *350*, 320−322.
(3) Fleming, R. M.; Rosseinsky, M. J.; Ramirez, A. P.; Murphy, D. W.; Tully, J. C.; Haddon, R. C.; Siegrist, T.; Tycko, R.; Glarum, H.; Marsh, P.; Dabbagh, G.; Zahurak, S. M.; Makhija, A. V.; Hampton, C. *Nature* **1991**, *352*, 701−703.
(4) Kortan, A. R.; Kopylov, N.; Glarum, S.; Gyorgy, E. M.; Ramirez, A. P.; Fleming, R. M.; Thiel, F. A.; Haddon, R. C. *Nature* **1992**, *355*, 529−532.
(5) Kortan, A. R.; Kopylov, N.; Glarum, S.; Gyorgy, E. M.; Ramirez, A. P.; Fleming, R. M.; Zhou, O.; Thiel, F. A.; Trevor, P. L.; Haddon, R. C. *Nature* **1992**, *360*, 566−568.
(6) Kortan, A. R.; Kopylov, N.; Özdas, E.; Ramirez, A. P.; Fleming, R. M.; Haddon, R. C. *Chem. Phys. Lett.* **1994**, *233*, 501−505.
(7) Kortan, A. R.; Kopylov, N.; Fleming, R. M.; Zhou, O.; Thiel, F. A.; Haddon, R. C. *Phys. Rev. B* **1993**, *47*, 13070−13073.
(8) Özdas, E.; Kortan, A. R.; Kopylov, N.; Ramirez, A. R.; Siegrist, T.; Rabe, K. M.; Bair, H. E.; Schuppler, S.; Citrin, P. H. *Nature* **1995**, *375*, 126−129.
(9) Chen, X. H.; Roth, G. *Phys. Rev. B* **1995**, *52*, 15534−15536.
(10) Krätschmer, W.; Lamb, L. D.; Fostiropoulos, K.; Huffman, D. R. *Nature* **1990**, *347*, 354−358.
(11) Mestres, J.; Duran, M.; Solà, M. *J. Phys. Chem.* **1996**, *100*, 7449−7454 and references therein.
(12) Vaughan, G. B. M.; Heiney, P. A.; Fischer, J. E.; Luzzi, D. E.; Ricketts-Foot, D. A.; McGhie, A. R.; Hui, Y. W.; Smith, A. L.; Cox, D. E.; Romanow, W. J.; Allen, B. H.; Coustel, N.; McCauley, J. P., Jr.; Smith, A. B., III *Science* **1991**, *254*, 1350−1352.
(13) Verheijen, M. A.; Meekes, H.; Meijer, G.; Bennema, P.; de Boer, J. L.; van Smaalen, S.; van Tendeloo, G.; Amelinckx, S.; Muto, S.; van Landuyt, J. *Chem. Phys.* **1992**, *166*, 287−297.
(14) Knupfer, M.; Poirier, D. M.; Weaver, J. H. *Phys. Rev. B* **1994**, *49*, 8464−8474.
(15) Sohmen, E.; Fink, J. *Phys. Rev. B* **1993**, *47*, 14532−14540.
(16) Imaeda, K.; Yakushi, K.; Inokuchi, H.; Kikuchi, K.; Ikemoto, I.; Suzuki, S.; Achiba, Y. *Solid State Commun.* **1992**, *84*, 1019−1024.
(17) Kobayashi, M.; Akahama, Y.; Kawamura, H.; Shinohara, H.; Sato, H. *Phys. Rev. B* **1993**, *48*, 16877−16880.
(18) Wang, Z. H.; Dresselhaus, M. S.; Dresselhaus, G.; Wang, K. A.; Eklund, P. C. *Phys. Rev. B* **1994**, *49*, 15890−15900.

10.1021/ja993881m CCC: $19.00
Published on Web 06/06/2000

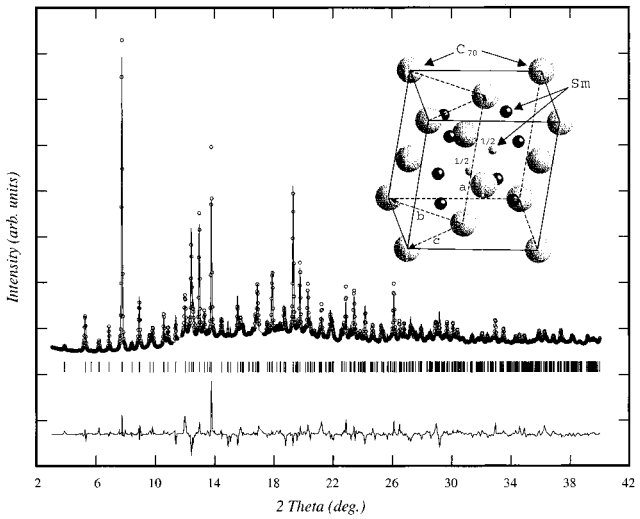

Figure 1. X-ray diffraction pattern of the sample Sm_3C_{70} collected with synchrotron radiation. The synchrotron beam was monochromatized to 1.0006 Å. The circles are experimental points and the solid line is a simulated result from the model of the monoclinic structure in space group *P*2. The schematic structure is shown in the inset. The allowed reflection positions are denoted by ticks.

reports have been presented of the stable phases of the C_{70} fullerides, especially their structural analysis. In this paper, we report two new stable phases of the C_{70} fullerides Sm_3C_{70} and Ba_3C_{70}, and give the first structural model for C_{70} fullerides. The structure of Ba_3C_{70} is derived from the A15 structure adopted by Ba_3C_{60}. Electronic transport properties were also studied. Different transport mechanisms are operative for Sm_xC_{70} fullerides with different values of *x*.

Experimental Section

Samples of Sm_xC_{70} ($x = 3$, 6) and Ba_3C_{70} were synthesized by reacting stoichiometric amounts of powders of Sm and C_{70}. A quartz tube with mixed powder inside was sealed under high vacuum of about 2×10^{-6} Torr. The samples of Sm_xC_{70} ($x = 3$, 6) and Ba_3C_{70} were calcined at 550 °C for 216 h, then cooled to room temperature in the furnace. It should be pointed out that the C_{70} was heated at 300 °C for 24 h under a vacuum on the order of $10^{-5}-10^{-6}$ Torr to remove the solvent before the reaction, and the X-ray diffraction profile of the starting C_{70} can be assigned to a hcp structure except for a small fcc phase. X-ray diffraction (XRD) measurements were carried out with synchrotron radiation at beam line BL 1B of the photon Factory of the National Laboratory for High Energy Physics (KEK−PF, Tsukuba). The synchrotron beam was monochromatized to 1.0006 Å. Simulation of the XRD patterns was carried out using Fullprof-98.[19] It is found that the fullerides Sm_3C_{70} and Ba_3C_{70} are very stable compounds. X-ray powder diffraction showed that the reaction reproducibly yielded single phase compounds.

To measure the resistivity, the mixed powder with stoichiometric composition was pressed into pellets, then fired as described above. Resistivity measurements were carried out using the four-probe method. Electrical contacts of less than 2 Ω resistance were established by silver paste. Preparation of samples and electrical contacts was carried out in a controlled argon glovebox where the oxygen and water vapor levels were maintained below a few parts per million.

Results and Discussion

Figure 1 shows the X-ray diffraction (XRD) pattern of the Sm_3C_{70} sample. All the observed peaks in the XRD pattern can be indexed to a monoclinic structure except for a few weak lines. Le Bail extracted lattice parameters of $a = 14.88(1)$ Å, $b = 10.09(1)$ Å, $c = 10.93(1)$ Å, and $\beta = 96.16(2)°$. This unite cell is derived by a slight deformation of the face-centered cubic structure of C_{70}. The lattice parameter of 14.88 Å along the *a*-axis is nearly the same as the lattice parameter of 14.93 Å for the C_{70} fcc structure,[13] while those along the *b*-axis and the *c*-axis are nearly the same as half of the diagonal in the *bc* plane for the fcc structure. There are no superlattice peaks in Sm_3C_{70}, in contrast with the cell doubling in $Sm_{2.75}C_{60}$ due to vacancy ordering.[8]

Table 1. Results of the Rietveld Refinement of Sm_3C_{70} within the Spherical Shell Model of C_{70} (Space Group *P*2)

atom	site	*x*	*y*	*z*	occupancy	*B*(A^2)
C_{70}(1)	1a	0.00000	0.00000	0.00000	1	0.16
C_{70}(2)	1d	0.50000	0.5000	0.5000	1	0.16
T Sm(1)	2e	0.223(3)	0.976(1)	0.539(3)	1	0.23
T Sm(2)	2e	0.258(3)	0.525(4)	0.002(4)	1	0.23
O Sm(3)	2e	0.596(4)	0.011(5)	0.260(3)	0.5	0.23
O Sm(4)	2e	0.092(3)	0.427(4)	0.399(3)	0.5	0.23

The above Le Bail fit simultaneously showed that there are only three possible space groups, namely, *P*2/*m*, *P*2, and *P*1. We checked these space groups with a Rietveld analysis within a spherical shell model of C_{70} and Fourier transformation. The *R*-factors of the refinement in *P*2/*m*, the space group of the highest symmetry, never decrease to less than 10%. Also, the Fourier transformation clearly showed that the Sm positions in the octahedral sites are not on the mirror plane, indicating that *P*2 is more likely. A Rietveld fit in *P*2 gave *R*-factors of $R_{wp} = 8.23\%$, $R_p = 6.88\%$, $R_I = 12.7\%$, $\chi^2 = 12.63$. The results of the refinement are displayed in Figure 1 by a solid line, and the parameters are listed in Table 1. In this analysis, only the positions of Sm^{2+} were refined, keeping all the other parameters unchanged including occupancy and thermal factors, since the Sm positions are the most dominant factors in the intensity distributions. Refinement of thermal factors and occupancies was unstable. The valence of the Sm ion was assumed to be Sm^{2+}, according to the divalent nature of Yb and Sm ions in Yb_xC_{60}[8] and Sm_xC_{60}.[9] The occupancy of the interstitial sites turned out to be more complicated than that of the well-known fcc structure of alkali-doped C_{60}. While the tetrahedral site is occupied by a single Sm ion in a conventional manner, there exist at least two stable Sm positions in the octahedral site. The absense of superlattice peaks indicates that the two sites are randomly occupied by Sm. Further refinement, most importantly the orientation of C_{70} molecules, could be possible, but the reliability of such analysis is extremely limited at the moment, partly because of insufficient sample quality. More detailed analysis, including the improvement of sample quality, is in progress.

It should be pointed out that the structure of Sm_3C_{70} seems to have nothing to do with the starting C_{70} structure. This is different from the case of K_xC_{70} reported by Kobayashi et al.,[17] in which the structure of K-doped C_{70} depended on the starting C_{70} structure. For highly Sm-doped C_{70} samples, the XRD patterns are different from those of Sm_3C_{70} with a large amorphous background, and the crystallinity is not good enough to identify them. So the X-ray diffraction patterns of Sm_6C_{70} are not presented.

Figure 2 shows the X-ray diffraction (XRD) pattern of the Ba_3C_{70} sample. It was found that most of the strong peaks could be indexed to the A15 structure with a lattice parameter of 11.74(1) Å. However, these strong peaks are split into two relative to the A15 structure adopted by Ba_3C_{60}. This suggests that the structure of Ba_3C_{70} is not cubic. Nearly all the strong peaks can be indexed by a tetragonal structure with lattice

(19) Fullprof, Rodriguez-Carvajal, J., Ed.; Laboratoire Leon Brillouin (CEA-CNRS), Version 3.5d, Oct. 1998.

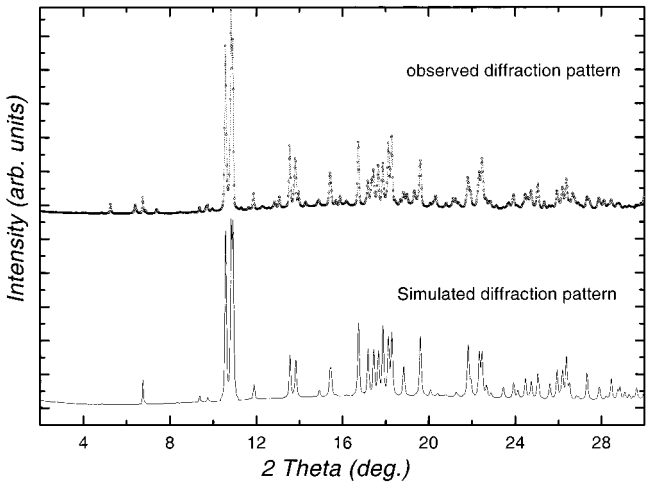

Figure 2. X-ray diffraction pattern of the sample Ba_3C_{70} collected with synchrotron radiation. The synchrotron beam was monochromatized to 1.0006 Å. The solid line is the calculated result from the distorted A15 structure with $a = b = 11.75(1)$ Å and $c = 12.23(1)$ Å in space group *Pmmm*.

parameters of $a = 11.75(1)$ Å and $c = 12.23(1)$ Å. Simulations of the X-ray diffraction data were carried out using FULLPROF-98 within the spherical shell model of C_{70}. The structural model is a distorted A15 structure. In the simulation, the position of Ba is the same as that of Ba in the A15 structure of Ba_3C_{60} and the C_{60} molecules in Ba_3C_{60} are replaced by C_{70} molecules. The C_{70} molecule is considered to be a spherical shell of charge. The solid line in Figure 2 is the calculated result from the model of orthorhombic structure with $a = b = 11.75(1)$ Å and $c = 12.23(1)$ Å in space group *Pmmm*. It is easily seen that the calculated relative intensity is nearly consistent with the observed results. These results definitely indicate that the structure of Ba_3C_{70} is derived from a distorted A15 structure adopted by Ba_3C_{60}. In Figure 2, many weak peaks cannot be indexed, especially at a low angle below 14°. All the observed weak peaks except for two peaks at angles of 5.2° and 6.4° can be indexed if the lattice parameters metioned above are doubled. Doubling the unit cell with a small distortion into the monoclinic structrue with $a = 23.55(1)$ Å, $b = 23.4(1)$ Å, $c = 24.51(1)$ Å, and $\beta = 94.03(2)°$ can index all diffraction peaks including the two peaks at 5.2° and 6.4°. In addition, the *R* factor rapidly decreases from 19% for the tetragonal structure to 8.9% for the monoclinic structure in the refinement of the lattice constants. Doubling of the lattice parameters for Ba_3C_{70} relative to the A15 structure could arise from the same Ba cation vacancy ordering, being similar to the case of $Yb_{2.75}C_{60}$ and $Sm_{2.75}C_{60}$.[8,9] Indeed, we have found a Ba cation vacancy in the Rietveld refinement process. The monoclinic symmetry in the Ba_3C_{70} and Sm_3C_{70} structures could arise from the C_{70} molecule orientational ordering. The structures of both Ba_3C_{70} and Sm_3C_{70} have a monoclinic symmetry, suggesting that the C_{70} fullerides have intrinsically lower symmetry than the C_{60} fullerides.

Figure 3a shows the temperature dependence of the resistivity of samples of Ba_3C_{70} and Sm_xC_{70} ($x = 3$, 6) and Ba_3C_{70}. No superconducting transition is observed at temperatures down to 4.2 K. The resistivity apparently decreases as the Sm concentration is increased. The sample Sm_3C_{70} shows strong semiconductor-like behavior, and the ratio $\rho(4.2K)/\rho(290K)$ is about 4300. The sample of Sm_6C_{70} shows a weak localization behavior at low temperature and the ratio $\rho(4.2K)/\rho(290K)$ is about 1.84. This is consistent with the band structure calculation. C_{70} has two low-lying unfilled levels: A_1'' and E_1'', which are

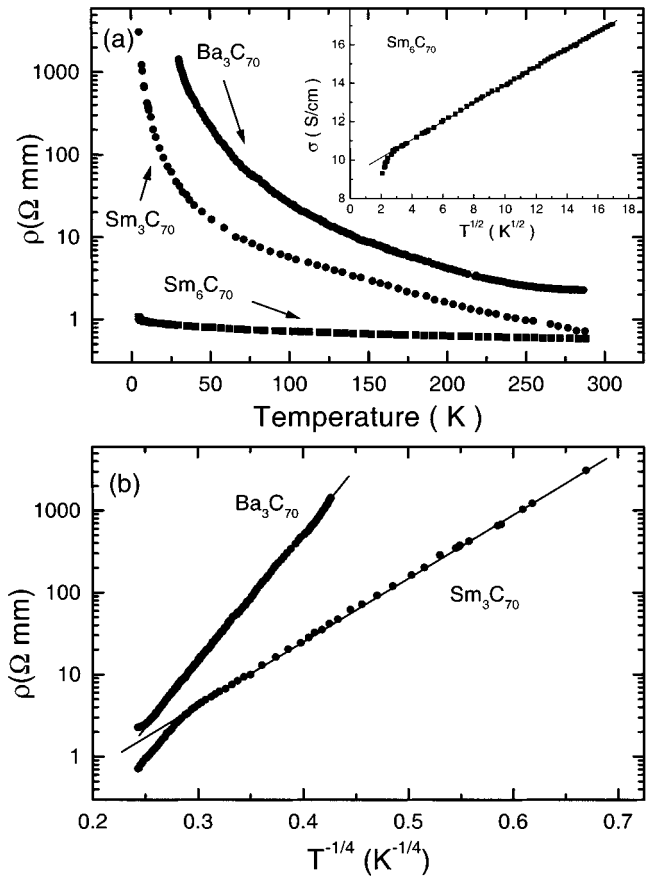

Figure 3. (a) The temperature dependence of resistivity for polycrystalline Sm_xC_{70} ($x = 3$, 6) and Ba_3C_{70}. The inset plots the same data as σ vs $T^{1/2}$ for Sm_6C_{70}. A straight line would be expected if the charge transport were dominated by a 3D weak localization and e−e interactions. (b) The same data are plotted as ln ρ vs $T^{-1/4}$ for Sm_3C_{70} and Ba_3C_{70}. A linear relation would be expected if the charge transport followed the 3D variable-range hopping theory.

singly and doubly degenerate, respectively.[20] One thus expects that Sm_3C_{70} is an insulator due to the complete filling of its lowest unoccupied molecular orbital (LUMO) bands. On the other hand, the room-temperature conductivity σ of Sm_xC_{70} fullerides is larger than the σ maximum of 2 S/cm in K_xC_{70} thin films reported by Haddon et al.,[2] in which σ initially increases with doping and reaches a maximum, but decreases with further doping. Imaeda et al. found that the spin concentration goes through two maxima as a function of doping.[16] However, no maximum of conductivity as a function of doping is observed in Sm_xC_{70}. It suggests that the K_xC_{70} system has a more abundant phase diagram than the Sm_xC_{70} system. Ba_3C_{70} also shows a strong semiconductor-like behavior. Its room temperature resistivity is nearly the same as that of Sm_3C_{70}, and the transport behavior is similar to that of Sm_3C_{70}.

The inset of Figure 3a plots the same data for Sm_6C_{70} as σ vs $T^{1/2}$. A linear relation would be expected in this plot if the transport were dominated by three-dimensional weak-localization and electron-electron interactions. For the sample Sm_6C_{70}, a straight line between 6 K and room temperature and a slight deviation from the line from 6 to 4.2 K are observed. This result suggests that Sm_6C_{70} is a weak localization system with electron-electron (e−e) interactions. This is similar to the case of the most conducting K_4C_{70} thin film and Sm_xC_{70} in which the transport is also described by weak localization and an e−e

(20) Saito, S.; Oshiyama, A. *Phys. Rev. B* **1991**, *44*, 11536−11539.

interaction model.[9,18] It suggests that there exists at least one metallic phase besides the insulating phase Sm_3C_{70} in the Sm_xC_{70} system, although it cannot be identified as yet.

Figure 3b plots the same data for Sm_3C_{70} and Ba_3C_{70} as ln ρ vs $T^{-1/4}$. A nearly linear relation is observed below 175 K for Sm_3C_{70}, and in the whole temperature measurement range for Ba_3C_{70}. That indicates that the resistivity of Sm_3C_{70} and Ba_3C_{70} at low temperature can be fit by the three-dimensional (3D) variable-range hopping formula $\rho(T) = \rho_0 \exp(T_0/T)^{1/4}$. It indicates that the transport is dominated by 3D variable-range hopping. These results indicate that the electronic structures of Sm_3C_{70} and Ba_3C_{70} are almost the same. The transport results of Sm_xC_{70} and Ba_3C_{70} are similar to those of Ba_xC_{60} film.[21] All of the compounds show a maximum in resistivity at $(AE)_3C_{60}$ (AE = Ca, Sr, Ba), corresponding to complete filling of the t_{1u} level. The highly doped C_{60} with alkaline-earth metals reach their lowest resistivities as a result of the population of the next lowest unoccupied molecular orbital of C_{60}.

Structural analysis shows that the fullerides Sm_3C_{70} and Ba_3C_{70} have monoclinic symmetry. This could be intrinsic to the C_{70} fullerides due to the molecular symmetry of C_{70}. Rosseinsky[22] has pointed out that fully ordered structures for C_{70} fullerides should have monoclinic symmetry. The low symmetry could be one important factor for no superconductivity being observed in the C_{70} fullerides. For C_{60} fullerides, superconductivity appears only in the structure with high symmetry. Theory has indicated that the orientational disorder required by the reported crystal symmetries will have a profound effect on properties.[23] In addition, the near-spherical shape and LUMO degeneracy of C_{60} are not present in C_{70}, and this may be a possible explanation for the differences in structural chemistry and electronic properties.

Conclusion

In summary, we present the synthesis, phase identification, and physical properties of a series of novel C_{70} fullerides Sm_xC_{70} ($x = 3, 6$) and Ba_3C_{70}. A simulation of the structure was made for Sm_3C_{70} and Ba_3C_{70}. We present the first structural model for C_{70} fullerides. Their transport properties were also studied by resistivity measurements. Structural analysis shows that Sm_3C_{70} and Ba_3C_{70} have monoclinic symmetry. This could be intrinsic to the C_{70} fullerides. There is as yet no detailed treatment of the C_{70}^{n-} orientation in any of these phases. We are working on this subject for Sm_3C_{70} and Ba_3C_{70}. The intrinsic low symmetry of C_{70} fullerides could be an important reason for the absence of superconductivity in C_{70} fullerides. The transport properties can be explained by a 3D variable-range hopping model for low-doped C_{70} fullerides, and by weak localization and e−e interaction theory for highly doped C_{70} fullerides.

Acknowledgment. We would like to acknowledge Y. Murakami for help in the synchrotron X-ray diffraction measurements. X.H.C. would like to thank the Inoue Foundation for Science for financial support. This work is supported by a grant from Natural Science Foundation of China. The work in Japan was supported by the JSPS "Future Program" (RFTF96P00104) and also by the Grant-in-Aid for Scientific Research on the Priority Area "Fullerenes and Nanotubes" by the Ministry of Education, Science, and Culture of Japan.

JA993881M

(21) Haddon, R. C.; Kochanski, G. P.; Hebard, A. F.; Fiory, A. T.; Morris, R. C.; Perel, A. S. *Chem. Phys. Lett.* **1993**, *203*, 433.

(22) Rosseinsky, M. J. *Chem. Mater.* **1998**, *10*, 2665−2685.

(23) Lu, J. P.; Gelfand, P. P. *Phys. Rev. B* **1995**, *51*, 16615−16618.